

REVIEW PAPER

Burn-back Equations for High Volumetric Loading Single-grain Dual-thrust Rocket Propellant Configuration

Himanshu Shekhar

High Energy Materials Research Laboratory, Pune-411 021
E-mail: himanshudrdo@rediffmail.com

ABSTRACT

Dual-thrust mode is adopted in solid propellant rocket propulsion through tailoring of burning area, nozzle, rocket motor chamber, propellant type, multiple propellant blocks. In the present study, mathematical formulation has been evolved for generation of burning surface area with web burnt for a simple central blind hole in a solid cylindrical propellant geometry with proper partial inhibition on external and lateral surfaces. The burn-back equation has been validated by static firing and parametric study was conducted to understand effect of various control geometrical parameters. The system is utilised for high volumetric loading, single propellant, single composition, single-chamber, single nozzle dual-thrust mode of burning profiles in rocket application.

Keywords: Dual-thrust, rocket propellants, web burnt, burning surface, boost-sustain

NOMENCLATURE

a	Burning rate coefficient
A_t	Throat area for the rocket motor
C^*	Characteristic velocity for the propellant composition
L_1	Depth of central blind hole in the propellant grain
L_2	Length of outer uninhibited portion of the propellant grain
L_g	Total length of the propellant grain
L_x	Auxiliary length for boost-to-sustain phase transition
m_d	Rate of discharge of combustion gases from nozzle
m_g	Rate of generation of combustion gases
n	Burning rate pressure exponent
P	Pressure inside rocket motor chamber
P_1, P_2	Constant parameters for grain configuration
r	Burning rate of solid propellant, $a \times P^n$
R_o	Outer radius of propellant grain
R_h	Radius of central hold in propellant grain
S	Surface area of propellant geometry
t	Time elapsed
T_1, T_2, T_3	Transitions lengths for web consumed in burning surface Eqns
w	Web burnt in the course of propellant combustion
α	Limiting angle for central spherical section
β	Limiting angle for outside surface of revolution
θ	Auxiliary angle for calculation and integration
ρ	Density of propellant

1. INTRODUCTION

Dual-thrust level (Boost-sustain) motors frequently provide a more effective delivery of impulse than those with an all-boost schedule, and are therefore specified for tactical rockets¹. Although neutrality of burning profile² is advocated through various geometrical configurations, like tubular, funnel³, star^{4,5,6}, finocyl^{7,8,9}, slotted tube¹⁰, anchor¹¹ etc, dual-thrust propulsion is always specified as an extension of two neutral burning propellants working in tandem. Preliminary estimate of dual-thrust grain configuration always starts with simplified rectangular dual-thrust profile model and the same was adopted for design of S-520 sounding rockets¹². Dual-thrust has two distinct levels of thrusts, achieved by different mechanisms like single-chamber and fixed nozzle, single-chamber and variable nozzle, double-chamber and single external nozzle¹³, double-chamber and multiple nozzle configurations.

In all modes except the first, there is considerable sub-optimal utilisation of chamber volume and enhancement in the inert hardware weight due to inert partitions, more empty volume, more insulation requirements, and lower propellant weight. The simplest configuration to get dual-thrust propulsion in rockets is achieved by single-chamber, single nozzle, single grain design and dual-thrust is obtained by geometrical configuration. Several methods have been described in literature for calculation of burning surface area evolved in course of burning¹⁴ but development of close-form, burn-back equation for each propellant geometry is a challenging task. Development of close-form solutions is effective to understand effect of various propellant grain control parameters for prediction of ballistic performance

of rockets. The configuration considered for the development of mathematical formulation and analysis is a partially inhibited simple cylindrical solid with blind cylindrical hole at one end.

2. CONFIGURATION DETAILS

Logical sequence in propellant grain design includes an understanding of the evolution of the classical shapes and certain aspects of grain topology from the purely morphological standpoint. Each grain configuration has inherent geometrical definition in terms of control dimensional parameters. Although grain design cannot proceed independent of system analysis and inert component design, but burn area evolution with web consumed in burning during propellant consumption can be treated independently for prediction of pressure-time, and subsequently, thrust-time profiles for a given configuration. Least sliver fraction, highest volumetric loading, minimum tail-off, conformance to ballistic requirements are constraints over which grain configuration is generally iterated. The propellant grain under consideration is depicted in Fig. 1.

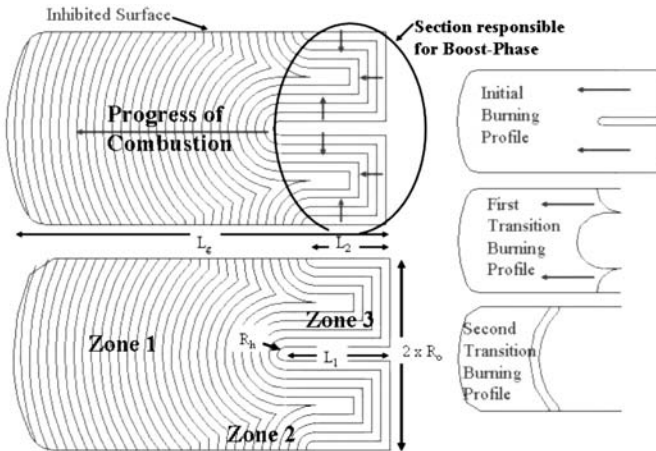


Figure 1. Salient parameters and burning surface regression of propellant geometry.

Propellant grain is characterised by five dimensional parameters only, contrary to most popular star configuration, where seven geometrical parameters are needed for their complete definition. The propellant configuration is truly axis-symmetric and burning surface evolution is three-dimensional in nature. Propellant grain radius (R_o) and total length (L_g) indicate overall dimension, while central hole radius (R_h), hole depth (L_1), and length of uninhibited outer surface (L_2) indicate essential features for evolution of dual-thrust burning pattern. Hole depth (L_1) is always kept more than the length of uninhibited lateral surface (L_2) to get smooth and gradual transition between two thrust phases. If such requirements are not met, sudden depressurisation may result in extinction of propellant burning surface. In this case, variation of burning surface area is responsible for dual-thrust mode.

In the initial phases of combustion, higher surface area is available for burning from the uninhibited end. It

gives higher pressure representing boost phase in thrust history. However, it gets consumed in the initial phase. This part is a combination of three surfaces – two cylindrical and one end face of a cylinder. This is represented as ‘Zone 3’ in Fig. 1. Junction of outer inhibited and uninhibited surfaces give rise to a concave burning cusp¹⁵ with centre at the interface. Because of cyclic symmetry, surface area is obtained as a surface of revolution of evolved spherical section about axis of the solid propellant grain. This gives rise to surface specified by ‘Zone 2’ in Fig. 1. As $L_1 > L_2$, a second transition in burning surface is observed where ‘Zone 2’ portion is completely consumed and burning surface area is entirely governed by central spherical section of the central blind hole (Zone 1).

The most significant part of burning pattern is imparted by the central hole, which acts as a solid of revolution, which is initially hemispherical, but later on, it becomes spherical with lower angles at the centre of spherical cross-section. This represents ‘Zone 1’ and is active throughout the combustion. Although in the initial phases, it contributes less in total burning profile, but later, low-thrust profile is the result of burning in this zone alone. This contributes significantly in sustainer phase burning.

The grain design is simple and processing of this geometry is very easy. It is observed that propellant can be manufactured by both casting and extrusion methods. Since geometric details of grain design are missing in most of the recent texts, analytical methods for determining burn surface area and port area as a function of burn distance for a variety of cylindrically-perforated solid rocket motor grains has been reviewed¹⁶. Star, long-spoke wagon wheel, dendrite grains are considered, but the simple grain design is not visited in open literature exclusively. Even in one of the recent literatures¹⁷, pseudo-dual-thrust burning profile was obtained from complicated finocyl-shaped geometry for propellant grain in ballistic evaluation motors. In this paper, mathematical formulation is developed for the relatively simple, partially inhibited cylindrical propellant grain with central blind hole to evolve burning surface area with web burnt.

3. MATHEMATICAL FORMULATION

Longitudinal section of propellant configuration is considered (Fig. 2) such that solid of revolution about central axis can give the entire propellant configuration. It is clear that first parameter namely $P_1 (= L_1 - L_2)$ represents difference of hole depth (L_1) and outer uninhibited surface length (L_2). Second parameter $P_2 (= \sqrt{R_o^2 + P_1^2})$ represents central distance between two spherical surfaces. Burning surface evolution is characterised by several transitions. Complete propellant grain consumption is characterised by web burnt of $(L_g - L_1 - R_h)$.

First transition of solid propellant grain is characterised by consumption of uninhibited section complete conversion of cup shape solid of revolution at the right into a single cylindrical surface. It is represented by web burn of T_1 and given by Eqn (1).

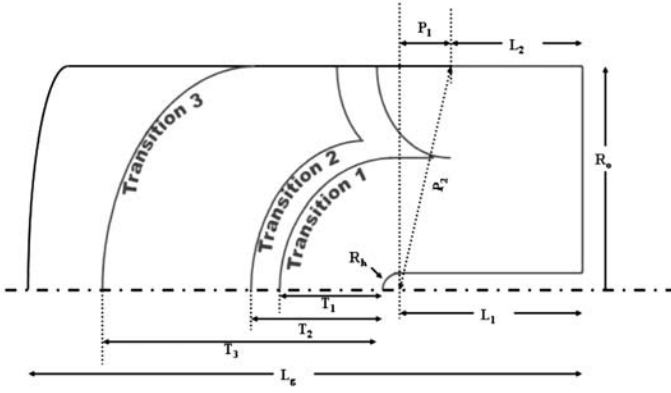


Figure 2. Salient parameters for burning surface evolution.

$$T_1 = (R_o - R_h)/2 \quad (1)$$

Second transition occurs when cylindrical surface is completely consumed and is represented by T_2 in the Fig. 2 and mathematically expressed as Eqn (2).

$$T_2 = [P_1^2 + (R_o - R_h)^2] / (2R_o - 2R_h) \quad (2)$$

Third transition, characterised by T_3 is represented by complete consumption of outer spherical surface. After this transition, entire burning surface is made of central spherical section only and is represented by Eqn. (3).

$$T_3 = (P_1^2 + R_o^2 - R_h^2) / (2R_h + 2P_1) \quad (3)$$

Most simple and well-developed formulation is possible for Zone 3 portion of the propellant configuration (Fig. 1), which is valid till transition T_1 is reached. For a given web burnt, w this surface is given by Eqn. (4).

$$S_3 = 2\pi(R_h + w)(L_2 - w) + 2\pi(R_o - w)(L_1 - w) + \pi(R_h + R_o)(R_o - R_h - 2w) \quad (4)$$

Between transitions T_1 and T_2 , this zone is reduced to a simple cylindrical section. Length of this cylindrical section (L_x) is given by Eqn (5).

After transition T_2 , this section does not contribute to the surface area. Surface area between transition T_1 and T_2 is given by Eqn (6).

$$L_x = P_1 - \sqrt{[(R_o - R_h)^2 + (2w + R_h - R_o)^2]} \quad (5)$$

$$S_3 = 2\pi(R_h + w) L_x \quad (6)$$

Zone 1 is a section of a spherical surface, with limiting angle given by α . On integration (Fig. 3), the surface area is calculated in terms of this control parameter (α). However, value of α varies with transition status. Variation of α with web burnt is given by Eqn (7).

$$S_1 = 2\pi(R_h + w)^2(1 - \cos \alpha)$$

where $\alpha = \pi/2$ for $w < T_2$

$$= \pi - \tan^{-1}\left\{\frac{R_o/P_1 - \cos^{-1}\left\{\frac{(R_h + w)^2 + P_2^2 - w^2}{2(R_h + w)P_2}\right\}}{(R_h + w)P_2}\right\}$$

for $T_2 < w < T_3$

$$= \sin^{-1}\left\{\frac{R_o}{R_h + w}\right\} \text{ for } T_3 < w < (L_g - L_1 - R_h) \quad (7)$$

Zone 2 is created at the external diameter of the grain

and is also in the form of a surface of revolution of a circular arc. But in this case, axis of revolution is offset in the direction opposite to the centre of curvature of the arc. This surface is governed by a limiting angle β (Fig. 3). This surface disappears, once transition T_3 is reached. The evolved surface is given by Eqn. (8).

$$S_2 = 2\pi w \{R_o \beta - w + w \cos \beta\},$$

where

$$\beta = \pi / 2 \text{ for } w < T_1$$

$$= \pi/2 - \sin^{-1}\{(P_1 - L_x)/w\} \text{ for } T_1 < w < T_2$$

$$= \sin^{-1}\left\{\frac{R_o - (R_h + w)\sin \alpha}{w}\right\} \text{ for } T_2 < w < T_3 \quad (8)$$

Total burning surface area is the summation of all the burning surface areas for three sections obtained using Eqns (4, 7, and 8). With mathematical formulation developed in this Section, burn area versus web burnt for the propellant configuration can be obtained.

When propellant combustion in rocket motor chamber occurs, combustion gases are evolved and mass balance equations for estimation of pressure are well reported¹⁸. Mass generation by combustion of propellant is given by Eqn. (9).

$$m_g = \rho \times r \times S = \rho \times a \times P^n \times S \quad (9)$$

At the same time gases are discharged from the nozzle also [Eqn. (10)].

$$m_d = P \times A_t \times g/C^* \quad (10)$$

For steady-state situation, mass generation [Eqn. (9)] is equal to mass discharge through the nozzle [Eqn. (10)]. This gives operating point or equation of pressure inside rocket motor chamber [(Eqn. 11)].

$$P = (a \times \rho \times C^* \times S/A_t \times g)^{1/(1-n)} \quad (11)$$

The calculation made using web increment from zero web to complete consumption of propellant grain and adequate web burnt steps. For each web, corresponding surface area is generated using equation. Using Eqn. (11),

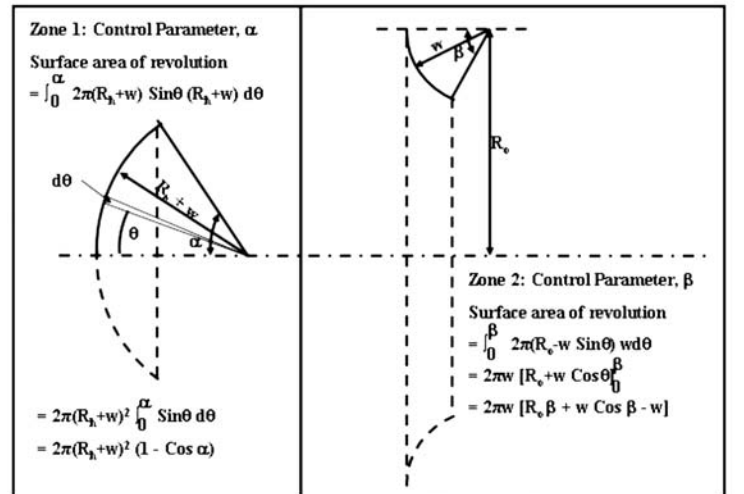


Figure 3. Surface of revolution for different zones.

for each generated surface area, pressure generated in rocket motor chamber is calculated. Since burning rate coefficient and burning rate pressure exponent are known for a given propellant, burning rate ($r = a \times P^n$) corresponding to each pressure is generated. Initially, both time (t) and web burnt (w) are zero. For each increment in web (Δw), pressure generated [Eqn. (11)] gives instantaneous burning rate and time increment is obtained using Eqn. (12). This time increment is added to the earlier time to get current time. This algorithm helps in generation of pressure-time profile.

$$\Delta t = \Delta w / (a \times P^n) \tag{12}$$

4. RESULTS AND DISCUSSION

To validate the mathematical formulation, a propellant grain with salient parameters as indicated in Table 1 is evaluated through static firing and pressure-time profile is recorded. Pressure-time profile is also predicted using mathematical formulation developed in Section 3. The superimposed curves are given in Fig. 4.

Predictions have been made without considering any ignition delay and tail-off portion obtained at the end of firing is also not included in the formulation. However, in static firing curve for boost phase, nature of curve, pressure, and time are exactly matching to the predicted curve. Pressure transition between the two phases is also matching. Pressure levels in sustainer phase are also matching for most of the duration. In actual static firing, grain regression deviates from ideal at the end of burning, and so, the tail-off portion is not matching. In fact in actual motor firing, combustion of propellant creates extra volume for combustion gases and near the end of propellant consumption, this

Table 1. Salient parameters for static firing

Parameter (unit)	Symbol	Value
Outer radius of propellant (mm)	R_o	54
Total length of propellant (mm)	L_g	213
Hole radius (mm)	R_h	4
Hole depth (mm)	L_1	59
Uninhibited length at outer dia (mm)	L_2	42
Propellant density (g/cc)	ρ	1.58
Characteristic velocity (m/s)	C^*	1380
Burn rate law (mm/s)	r	$6.6491 \times P^{0.1052}$
Throat area of rocket motor (m ²)	A_t	54.63

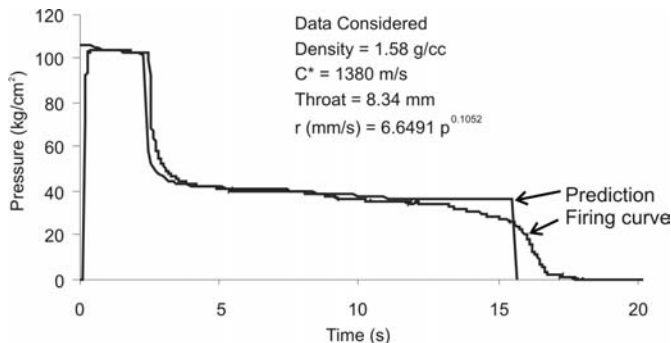


Figure 4. Validation of developed formulation by static firing.

part is significant. Since formulation is based on steady-state condition [Eqn. (11)], near end of combustion, actual pressure realised is less than the predicted. Lowering of pressure enhances burning time also. The close matching of firing curve and prediction ensures correctness of mathematical close-form burn-back equation for the configuration.

To understand effect of each of the salient parameters, parametric study was also conducted for the given configuration. Since mathematical formulation developed in this study is restricted to burning surface area calculations, comparison and effects of various parameters are also depicted in burning area versus web burnt profiles only. It must be noted that pressure-time or thrust-time profiles are in fact scaled versions of burning surface area and web-burnt profiles. For different propellant properties, suitable pressure-time and thrust-time profiles can be extracted.

For parametric study, outer radius (R_o) of the propellant is considered as base parameter. Total length (L_g) to outer radius ratio (L_g/R_o) of the propellant grain is taken as 5. Variation of volumetric loading fraction is plotted against ratio of L_1/R_o for different R_h/R_o in Fig. 5. It is clear that as L_1/R_o increases, volume loading fraction reduces. A similar trend was observed with increase in R_h/R_o . However even for a very unlikely hypothetical case of hole depth fraction equal to 1.5 and hole radius fraction of 0.47, volumetric loading fraction is > 90 per cent. It clearly indicates that prime requirement of high loading fraction is accomplished by this propellant grain configuration.

Effect of hole radius fraction (R_h/R_o) on the burning surface area versus web-burnt profile was also studied. The variations are plotted as Fig. 6. It is clear that variation of radius of hole alone does not affect sustainer part or low-burning area part of the curve. However, booster phase is significantly affected. Higher hole radius indicates higher hole radius and ultimately higher initial burning surface area is available. However, burning time shows a reverse trend and higher hole radius invariably gives lower boost phase time. Transition is also smooth for lower value of hole radius.

In the propellant configuration, two important length parameters are defined. One is hole depth (L_1) and the other is length of uninhibited portion at the outer periphery of the propellant grain (L_2). For the configuration under consideration,

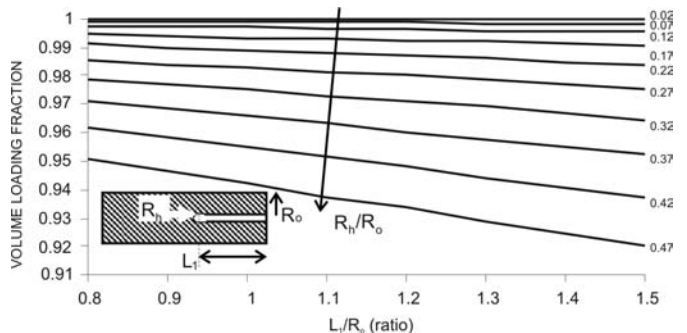


Figure 5. Variation of volume loading fraction.

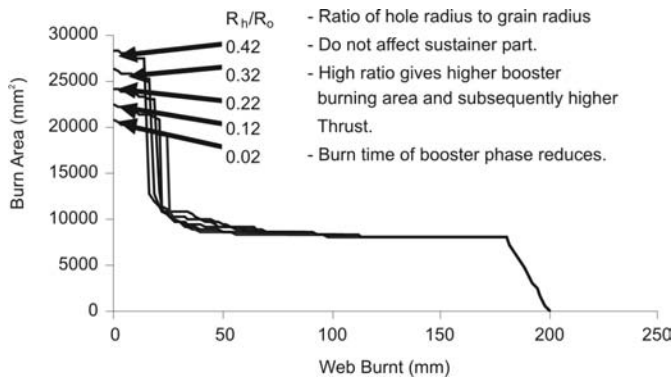


Figure 6. Effect of varying hole radius fraction.

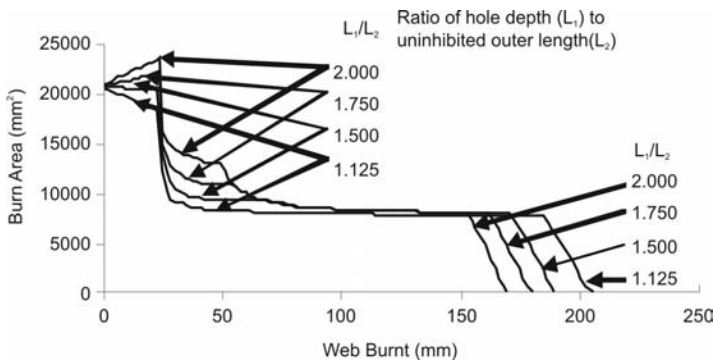


Figure 7. Variation in performance profile with length ratio.

L_1 is always $> L_2$. Effect of ratio of these lengths on performance prediction curves was also explored. As length ratio (L_1/L_2) increases, boost phase profile changes from regressive to progressive profile. Sudden drop in burning surface area occurs almost at the same duration. At high length ratio, total burning time reduces. Alternately, sustainer phase burning time reduces for higher length ratio. For smaller length ratio, transition was more smooth. At higher length ratio, tendency to form a secondary higher burning area was observed. Single-chamber, single grain, single nozzle, single propellant configuration was explored for realisation of dual-thrust burning profile. Achievement of dual-thrust by configuration alone is established. As the number of parameters are less, better control and smooth repeatable performance is expected from the grain under consideration.

5. CONCLUSION

Close-form, burn-back equation has been developed for performance prediction of partially inhibited solid cylindrical propellant grain. With partial inhibition and a blind hole at centre is capable of developing dual-thrust by burning surface area alone. The grain configuration is simple and easy to manufacture. The burning surface profile is three-dimensional and is analysed with integration of infinitesimal burning areas. Parametric studies were carried out and high volumetric loading is expected from designed propellant configuration. Effect of variations in hole parameters on burning area versus web-burnt profile was studied for completeness. The developed mathematical formulation is validated by conducting static evaluation of grain conforming

to the considerations of the propellant grain under investigation. The mathematical formulation is easily adaptable for any dual-thrust propulsion.

REFERENCES

1. Solid propellant grain design and internal ballistics. NASA Space Vehicle Design Criteria (Chemical Propulsion). NASA Report No. NASA SP-8076, March 1972.
2. Krishnan, S. Design of neutral burning star grains. *Journal of Spacecraft*, 1975, **12**(1), 60-62.
3. Shekhar, Himanshu. Design of funnel port tubular propellant grain for neutral burning profile in rockets. *Def. Sci. J.*, 2009, **59**(5), 494-98.
4. Ricciardi, Andrea. Generalized geometric analysis of right circular cylindrical star perforated and taper grains. *Journal of Propulsion*, 1992, **8**(1), 51-58.
5. Shekhar, Himanshu. Modelling of burning surface regression of taper convex star propellant grain. *Def. Sci. J.*, 2000, **50**(2), 207-11.
6. Shekhar, Himanshu. Parametric studies on star port propellant grain for ballistic evaluations. *Def. Sci. J.*, 2005, **55**(4), 459-69.
7. Kuo, K.K.; Kokal, R.A.; Paulauskas, M.; Alaksin, P. & Lee, L.S. Flame spreading phenomena in fin slots of solid rocket propellants. *J. Propul. Power*, 2001, **17**(5), 1005-011.
8. Shekhar, Himanshu. Close-form solution for burning surface evolution and performance prediction of finocyl shaped propellant grain. In International Autumn Seminar on Propellant, Explosives and Pyrotechnics (2007 IASPEP), Nan Yang Hotel, Xi'an, China, 23-26 October 2007. pp. 907-911.
9. Nissar, Khurran & Guozhu, Liang. Design and optimization of three-dimensional finocyl grain for solid rocket motor. In 44th AIAA/ASME/SAE/ASEE Joint Propulsion Conference and Exhibits, Hartford, CT, 21-23 July 2008. AIAA Paper No. AIAA-2008-4696.
10. Hartfield, Roy J.; Burkhalter, John E.; Jerkins, Rhonald M. & Witt, Jay. Analytical development of a slotted-grain solid rocket motor. *J. Propul. Power*, 2004, **20**(4), 690-94.
11. Umbel, Matthew R. An exact geometric analysis of the generalized anchor grain configuration. In 44th AIAA/ASME/SAE/ASEE Joint Propulsion Conference and Exhibits, Hartford, CT, 21-23 July 2008. AIAA Paper No. AIAA 2008-4697.
12. Matsuo, H.; Kohno, M.; Onoda, J.; Kawashima, T.; Murakami, T. & Onojima, N. Development of the S-520 single-stage sounding rocket. *Acta Astronautica*, 1982, **9**(10), 631-35.
13. Manda, Leo J. Boost-Phase equilibrium pressures in a dual-thrust solid-propellant rocket motor. *J. Spacecraft Rockets*, 1965, **2**(4), 607-09.
14. Wilcox, Michael A.; Brewster, M. Quinn; Tang, K.C. & Stewart, D. Scott. Solid propellant grain design and

- burnback simulation using a minimum distance function. *J. Propul. Power*, 2007, **23**(2), 465-75.
15. Epstein, L. Ivan. The design of cylindrical propellant grains. *Journal of Spacecraft*, 1956, **26**(9), 757-59.
 16. Hartfield, Ray; Jenkins, Rhonald; Burkhalter, John & Foster, Winfred. A review of analytical methods for solid rocket motor grain analysis. In 39th AIAA/ASME/SAE/ASEE Joint Propulsion Conference and Exhibits, Huntsville, Alabama, July 20-23, 2003. AIAA Paper No. AIAA 2003-4506.
 17. Puskulcu, G. & Ulas, A. 3-D Grain burnback analysis of solid propellant rocket motors: Part 1 – Ballistic motor tests. *Aero. Sci. Technol.*, 2008, **12**, 579-84.
 18. Solid rocket propulsion technology. Alain Davenas, Pergamon Press, UK, 1993.

Contributor



Dr Himanshu Shekhar received PhD from University of Pune and MTech (Mechanical Engineering) from IIT, Kanpur. Presently he is working as Joint Director at HEMRL (DRDO), Pune. He has been associated with advanced solid rocket propellants for the last 15 years. It includes development of infrastructure for solid rocket propellant processing, processing of solid rocket propellants, Mechanical properties evaluation, structural analysis and performance prediction of solid rocket propellants. He has 30 papers in peer reviewed journals and an equal number of publications in seminar and conference proceedings.